

*Supporting information for the paper:*

# A Stable, Cationic, Mononuclear Pt(III) Complex Stabilised by Bulky N-Heterocyclic Carbenes

Orestes Rivada-Wheelaghan,<sup>a</sup> Manuel A. Ortúñoz,<sup>b</sup> Sergio E. García-Garrido,<sup>c</sup> Josefina Díez,<sup>c</sup> Pablo J. Alonso,<sup>d</sup> Agustí Lledós,\*<sup>b</sup> Salvador Conejero\*<sup>a</sup>

<sup>a</sup>*Instituto de Investigaciones Químicas, Departamento de Química Inorgánica, CSIC, Universidad de Sevilla, Avda. Américo Vespucio no 49, 41092 Sevilla, Spain.*

<sup>b</sup>*Departament de Química, Universitat Autònoma de Barcelona, 08193 Cerdanyola del Vallès, Spain.*

<sup>c</sup>*Departamento de Química Orgánica e Inorgánica, Universidad de Oviedo, C/ Julián Clavería 8, 33006 Oviedo, Spain.*

<sup>d</sup>*Instituto de Ciencia de Materiales de Aragón (ICMA), Universidad de Zaragoza and CSIC, C/ Pedro Cerbuna 12, 50009, Zaragoza, Spain.*

## **Contents:**

1. General .....	S2
2. Synthesis and spectroscopic and analytical data for new compounds .....	S2
3. Cyclic voltammetry studies .....	S5
4. Computational details .....	S5
5. SOMO of complex $[Pt(C_6Cl_5)]^-$ .....	S6
6. Cartesian coordinates of DFT-optimised complexes .....	S6
7. EPR studies .....	S9
8. Magnetic measurements .....	S12
9. X-Ray Crystal Structure Determination of Complexes 2 and 3. ....	S15
10. References .....	S18

Crystallographic data are also deposited with Cambridge Crystallographic Data Centre. Copies of the data (2, 3: CCDC 969273 and 969274) can be obtained free of charge via [www.ccdc.cam.ac.uk/data\\_request/cif](http://www.ccdc.cam.ac.uk/data_request/cif), by e-mailing [data\\_request@ccdc.cam.ac.uk](mailto:data_request@ccdc.cam.ac.uk), or

by contacting Cambridge Crystallographic Data Centre, 12, Union Road, Cambridge CD 1EZ, UK; fax +44 1223 336033.

### 1. General

Microanalyses were performed by the Microanalytical Service of the Instituto de Investigaciones Químicas (Sevilla, Spain). The NMR instruments were Bruker DRX-500, DRX-400 and DPX-300 spectrometers. Spectra were referenced to external SiMe<sub>4</sub> ( $\delta$  0 ppm) using the residual protio solvent peaks as internal standards (<sup>1</sup>H NMR experiments) or the characteristic resonances of the solvent nuclei (<sup>13</sup>C NMR experiments). Spectral assignments were made by routine one- and two-dimensional NMR experiments where appropriate. All manipulations were performed under dry, oxygen-free argon, following conventional Schlenk techniques. [PtMeI(IPr)<sub>2</sub>]<sup>1</sup> and NaBAr<sup>F</sup><sup>2</sup> were prepared according to literature procedures.

### 2. Synthesis and spectroscopic and analytical data for new compounds

#### 2.1 Synthesis of complex [PtI<sub>2</sub>(IPr)<sub>2</sub>] (2)

0.9 ml (0.18 mmol) of a freshly prepared 0.2 M solution of I<sub>2</sub> in CH<sub>2</sub>Cl<sub>2</sub> were added to a solution of complex [PtMeI(IPr)<sub>2</sub>] (0.2 g, 0.179 mmol) in 3 mL of CH<sub>2</sub>Cl<sub>2</sub> at r.t. The solution was stirred for 30 min and the solvent removed under vacuum to obtain a dark-yellow solid. Purification was achieved by chromatography column (pentane to CH<sub>2</sub>Cl<sub>2</sub>) to yield a yellow solid that can be further purified if necessary by slow diffusion from concentrated solutions in CH<sub>2</sub>Cl<sub>2</sub> into diethyl ether (1:10) (218 mg, 99% yield).

**<sup>1</sup>H NMR (400 MHz, C<sub>6</sub>D<sub>6</sub>, 25 °C):**  $\delta$  7.36 (t, <sup>3</sup>J<sub>H,H</sub> = 8.0 Hz, 4H; Ph-CH<sub>p</sub>), 7.08 (d, <sup>3</sup>J<sub>H,H</sub> = 8.0 Hz, 8H; Ph-CH<sub>m</sub>), 6.84 (s, 4H; =CH), 3.23 (sept, <sup>3</sup>J<sub>H,H</sub> = 7.0 Hz; 8H; CH(CH<sub>3</sub>)<sub>2</sub>), 0.95, 0.89 (d, <sup>3</sup>J<sub>H,H</sub> = 7.0 Hz, 24H each; CH(CH<sub>3</sub>)<sub>2</sub>).

**<sup>13</sup>C{<sup>1</sup>H} (100 MHz, C<sub>6</sub>D<sub>6</sub>, 25 °C):**  $\delta$  163.3 (Pt=C), 146.3 (C<sub>q</sub>, Ph-C<sub>o</sub>), 136.8 (C<sub>q</sub>-N), 129.5 (Ph-CH<sub>p</sub>), 123.9 (Ph-CH<sub>m</sub>), 124.6 (=CH), 28.5 (CH(CH<sub>3</sub>)<sub>2</sub>), 27.8, 23.3 (CH(CH<sub>3</sub>)<sub>2</sub>).

**Elemental analysis calcd (%)** for C<sub>54</sub>H<sub>72</sub>I<sub>2</sub>N<sub>4</sub>Pt: C 52.90, H 5.92, N 4.57; **found** C 52.8, H 5.9, N 4.5.

#### 2.2 Synthesis of complex [PtI<sub>2</sub>(IPr)<sub>2</sub>][BAr<sup>F</sup>] (3)

0.1 g of complex **2** (0.082 mmol) and 72 mg of NaBAr<sup>F</sup> (0.082) were dissolved in 2 mL of CH<sub>2</sub>Cl<sub>2</sub>. Then, 2 mL of a freshly prepared solution of I<sub>2</sub> 0.02 M were added at r.t. The solution was stirred for 1 h observing a color change from yellow to deep blue. The solvent was then removed under vacuum and the remaining blue solid was washed with pentane (2 x 2 ml). The solid was re-dissolved in 2 mL of CH<sub>2</sub>Cl<sub>2</sub>, cooled to -20 °C and filtered via canula. Evaporation of the solvent lead to a blue solid than can be crystallized by slow diffusion from concentrated solutions in CH<sub>2</sub>Cl<sub>2</sub> into pentane (1:10) (120 mg, 70 % yield). Complex **3** can be stored at 5 °C indefinitely without noticeable decomposition.

**<sup>1</sup>H NMR (500 MHz, C<sub>6</sub>D<sub>6</sub>, 25 °C):** δ 7.92 (br, 24H), 7.76 (s, 8H, CH-BAr<sup>F</sup>), 7.63 (s, 4H, CH-BAr<sup>F</sup>), 4.13 (br, 4H), 2.08 (br, 8H), 1.24 (br, 4H), -0.60 (br, 24H), -7.27 (br, 8H).

**<sup>13</sup>C{<sup>1</sup>H} (125 MHz, C<sub>6</sub>D<sub>6</sub>, 25 °C):** δ 23.0 (br, CH<sub>aliphatic</sub>), 35.7 (br, CH<sub>aliphatic</sub>), 74.0 (br, CH<sub>aliphatic</sub>), 119.1, 122.6, 124.9, 133.0, 135.4 (br, CH<sub>aromatic</sub> and =CH), 117.4 (s, CH<sub>p</sub>-BAr<sup>F</sup>), 124.2 (q, J<sub>C,B</sub> = 272.5 Hz, CF<sub>3</sub>-BAr<sup>F</sup>), 129.2 (d, J<sub>C,B</sub> = 32.2 Hz, CH<sub>m</sub>-BAr<sup>F</sup>), 135.1 (C<sub>q</sub>, C<sub>o</sub>-BAr<sup>F</sup>), 162.1 (q, J<sub>C,B</sub> = 49.8 Hz, C<sub>ipso</sub>-BAr<sup>F</sup>). (Carbene signals of the IPr ligand were no detected).

**Elemental analysis calcd (%)** for C<sub>86</sub>H<sub>84</sub>BF<sub>24</sub>I<sub>2</sub>N<sub>4</sub>Pt: C 49.44, H 4.05, N 2.68;  
**found** C 49.4, H 4.4, N 2.6.

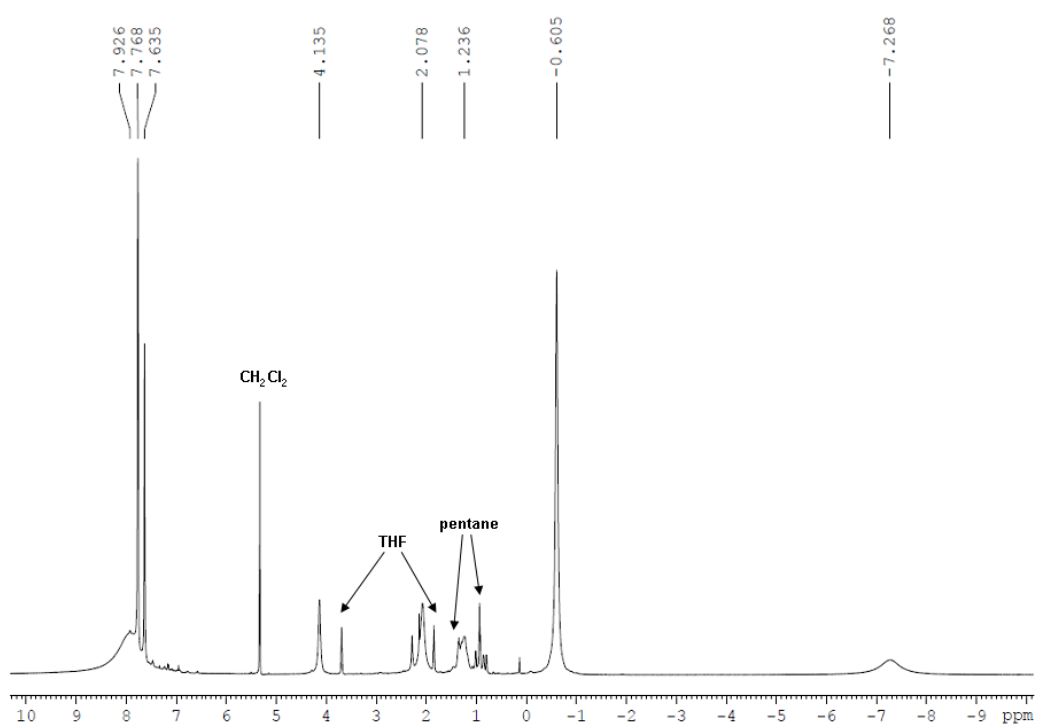


**Fig. S1**  $^1\text{H}$  NMR of complex **3** in  $\text{CD}_2\text{Cl}_2$ .

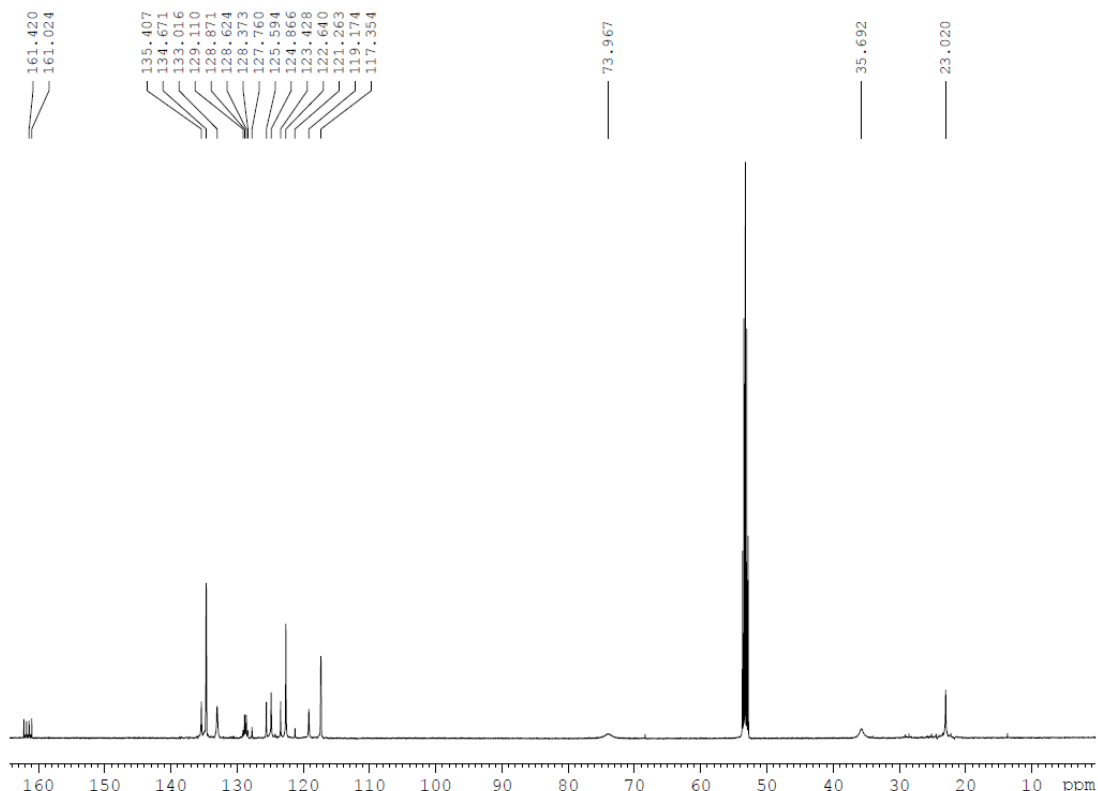


**Fig. S2**  $^{13}\text{C}\{^1\text{H}\}$  NMR of complex **3** in  $\text{CD}_2\text{Cl}_2$ .

### 3. Cyclic voltammetry studies

Electrochemical data was recorded on an ECO CHEMIE BV ( $\mu$ -Autolab Type III) electrochemical workstation and supporting software. Cyclic Voltammetry (CV) measurements were carried out with a three-electrode system. The working electrode was a 3 mm diameter glassy working carbon electrode, the counter electrode was a platinum spiral, and the reference electrode was an Ag/Ag<sup>+</sup> system. The working electrode was polished on 0.3  $\mu\text{m}$  diameter alumina on a Microcloth, followed by washing in dry dichloromethane prior to recording each voltammogram. In a typical experiment, 0.01 mmol of the complex was dissolved under a nitrogen atmosphere in 10 mL of freshly distilled and deoxygenated dichloromethane containing 0.383 g of pure [<sup>7</sup>Bu<sub>4</sub>N][PF<sub>6</sub>] (1 mmol) as supporting electrolyte. Data were gathered at room temperature (22 ± 2 °C) with a sweep rate of 0.2 V s<sup>-1</sup>.

For complex [PtI<sub>2</sub>(IPr)<sub>2</sub>] (**2**) the formal potential ( $E^\circ$ ) obtained was 0.730 V. This formal CV potential  $E^\circ$  is referenced relative to potential of the [Cp<sub>2</sub>Fe]–[Cp<sub>2</sub>Fe]<sup>+</sup> couple ( $E^\circ = 0.261$  V) run under identical conditions to that described for complex **2** ( $E^\circ = E^\circ([\text{PtI}_2(\text{IPr})_2]^+/\text{[PtI}_2(\text{IPr})_2]) - E^\circ([\text{Cp}_2\text{Fe}]^+/\text{[Cp}_2\text{Fe}])$ ).<sup>3</sup>

### 4. Computational details

All calculations were performed at the DFT level by means of the BHLYP functional<sup>4</sup> as implemented in Gaussian 09.<sup>5</sup> Calibration calculations on Cu<sup>+2</sup> open-shell complexes have shown that functionals with a large amount of exact exchange, as BHLYP, give results in good agreement with the CCSD(T) ones.<sup>6</sup> Pt and I atoms were described using scalar-relativistic Stuttgart-Dresden SDD pseudopotentials<sup>7</sup> with their associated double- $\zeta$  basis set, complemented with a set of f-polarisation functions.<sup>8</sup> The 6-31G\*\* basis set was used for H,<sup>9</sup> C, N, and Cl atoms.<sup>10</sup> Diffuse functions were added for Cl atoms.<sup>11</sup> The structures of the species were fully optimised without any symmetry restriction. The calculation of the Hessian matrix confirmed the structures corresponded with minima. Natural Orbitals (NOAB keyword) and Mulliken spin densities were computed as implemented in Gaussian 09.<sup>5</sup>

## 5. SOMO of complex $[\text{Pt}(\text{C}_6\text{Cl}_5)_4]^-$

In agreement with EPR experimental findings,<sup>12</sup> the computed SOMO of  $[\text{Pt}(\text{C}_6\text{Cl}_5)_4]^-$  displays a  $\text{dz}^2$  orbital centred on the platinum atom. No delocalisation across the ligands is observed.

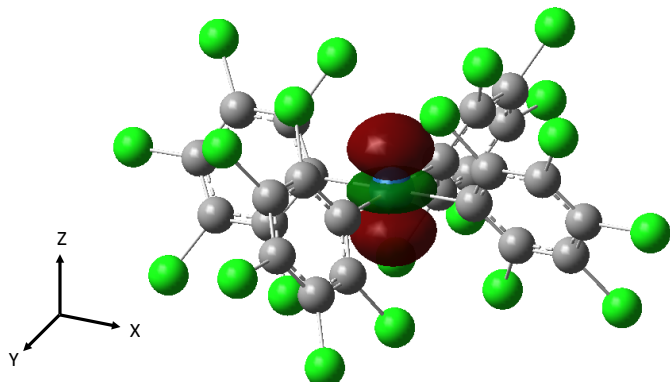


**Fig. S3** Calculated SOMO of the DFT-optimised  $[\text{Pt}(\text{C}_6\text{Cl}_5)_4]^-$  anion (isovalue 0.05).

## 6. Cartesian coordinates of DFT-optimised complexes

### $[\text{Pt}^{\text{II}}] \mathbf{2}$

Pt	0.000122	0.000050	0.000001	C	-0.651432	-4.235833	0.151319
I	0.000553	0.001529	2.673595	C	-2.919545	-2.379965	-1.908549
C	-0.000331	-2.076148	0.001205	C	3.647259	1.357537	-2.783222
C	0.000508	2.076241	-0.001240	C	3.148340	-3.794056	2.454312
N	-1.042697	2.915143	-0.251291	C	-3.146666	3.797171	2.450558
N	1.044070	2.915055	0.247553	C	0.649898	-4.236301	-0.145866
N	1.042838	-2.915391	-0.247802	C	-3.645793	1.363447	2.782784
C	1.940478	3.276236	3.031640	C	-5.067222	2.167196	-1.204125
C	2.837505	2.769891	1.913787	C	1.938865	-3.276649	-3.032082
C	-2.131689	4.780579	-3.245380	C	4.638578	-2.075034	0.105076
C	2.413554	-2.609540	-0.585537	C	5.067023	-2.169227	-1.203433
C	3.313178	-2.316751	0.448390	C	2.129942	-4.784753	-3.239881
C	2.414685	2.608625	0.585164	I	-0.000160	-0.001385	-2.673584
C	-2.836828	2.768321	-1.916717	N	-1.043852	-2.914625	0.251364
C	-2.180317	2.558920	-4.367451	C	-2.414492	-2.607706	0.588442
C	3.314077	2.315273	-0.448803	C	-3.313744	-2.315862	-0.446079
C	2.919283	-2.378675	1.911027	C	-2.837500	-2.766991	1.917246
C	-0.649702	4.236192	-0.151367	C	-3.646919	-1.362000	-2.782115
C	-3.312646	2.317199	0.446696	C	-3.149078	-3.796004	-2.449933
C	-1.940100	3.272803	-3.035650	C	-1.940697	-3.271788	3.035977
C	2.920097	2.377167	-1.911420	C	-4.639080	-2.072932	-0.103378
C	-2.918050	2.381023	1.909071	C	-4.178757	-2.527139	2.197059
C	5.067969	2.167022	1.202906	C	-5.067841	-2.165049	1.205176
C	2.132336	4.784272	3.239228	C	-2.180453	-2.557901	4.367855
C	-2.413542	2.608779	-0.588032	C	-2.132682	-4.779519	3.245659
C	0.651670	4.236126	0.145631	H	-1.398353	-2.830560	5.071800
C	2.836202	-2.770899	-1.914210	H	-2.166414	-1.481297	4.251352
C	3.150165	3.792251	-2.455056	H	-3.128458	-2.848823	4.814313
C	-4.178253	2.529025	-2.196205	H	-1.479436	-5.133690	4.039668
C	-4.638159	2.074797	0.104311	H	-3.158147	-4.997961	3.534901
C	2.178765	-2.564624	-4.364941	H	-1.912582	-5.358057	2.354993
C	4.178735	2.530536	2.194138	H	-0.909643	-3.090617	2.752887
C	4.177534	-2.532193	-2.194632	H	-4.531006	-2.630964	3.208643
C	4.639380	2.072911	-0.105562	H	-6.101134	-1.977510	1.449713
C	3.647289	-1.359796	2.783004	H	-5.345912	-1.826793	-0.876056
C	2.180017	2.564243	4.364578	H	-1.863202	-2.158520	-1.987401
				H	-3.564280	-0.359089	-2.378379
				H	-3.204975	-1.358807	-3.774533

H	-4.701741	-1.602962	-2.897597	N	-1.051983	2.924665	-0.221319
H	-2.580723	-4.539058	-1.897827	N	-1.049159	-2.925638	0.221476
H	-4.200842	-4.068178	-2.389731	C	-2.021801	3.194304	-2.988635
H	-2.846228	-3.853529	-3.492894	C	-2.880445	2.689207	-1.840331
H	-1.341157	-5.038658	0.296365	C	2.257677	4.691891	3.219974
H	1.339316	-5.039597	-0.289760	C	-2.427036	-2.595967	0.514691
H	0.907974	-3.094542	-2.748984	C	-3.295387	-2.335668	-0.553775
H	1.909645	-5.362039	-2.348452	C	-2.429543	2.593726	-0.514574
H	1.476359	-5.139537	-4.033338	C	2.878578	2.689780	1.841895
H	3.155231	-5.004150	-3.529024	C	2.269394	2.450397	4.305445
H	3.126481	-2.856748	-4.811231	C	-3.297746	2.332695	0.553834
H	1.396329	-2.837683	-5.068358	C	-2.879813	-2.488941	-2.004618
H	2.165466	-1.487858	-4.249845	C	0.653386	4.244775	0.134657
H	4.529518	-2.637594	-3.206147	C	3.295091	2.335670	-0.552765
H	6.100371	-1.982611	-1.448440	C	2.020124	3.193321	2.991019
H	5.345710	-1.828217	0.877267	C	-2.882411	2.486267	2.004712
H	1.863052	-2.156699	1.989830	C	2.878993	2.490379	-2.003312
H	3.205592	-1.355049	3.775526	C	-5.077052	2.057463	-1.053694
H	4.702046	-1.601018	2.898543	C	-2.259746	4.693060	-3.215982
H	3.564948	-0.357409	2.377910	C	2.427175	2.595184	0.516253
H	2.845705	-3.849993	3.497420	C	-0.657267	4.244340	-0.130732
H	2.579527	-4.537623	1.903364	C	-2.877946	-2.691757	1.840431
H	4.199971	-4.066776	2.394244	C	-3.202779	3.904534	2.492090
H	3.564259	0.355322	-2.377838	C	4.217223	2.398909	2.081646
H	3.205427	1.352835	-3.775684	C	4.620467	2.045431	-0.249450
H	4.702173	1.597972	-2.898962	C	-2.268141	-2.454446	4.304017
H	1.863693	2.155968	-1.990081	C	-4.218811	2.397749	-2.080899
H	4.202001	4.064211	-2.395130	C	-4.216548	-2.401304	2.080910
H	2.847496	3.848167	-3.498155	C	-4.622827	2.041934	0.249703
H	2.581942	4.536368	-1.904244	C	-3.523294	-1.459921	-2.932036
H	4.530845	2.635856	3.205616	C	-2.270426	2.452773	-4.303977
H	6.101238	1.979897	1.447858	C	0.657403	-4.244135	-0.134771
H	5.346323	1.825647	-0.877783	C	2.881922	-2.488105	2.003056
H	0.909484	3.094641	2.748591	C	-3.525240	1.456770	2.932058
H	1.397741	2.837811	5.067974	C	-3.199104	-3.907444	-2.492024
H	2.166127	1.487470	4.249608	C	3.197623	3.909531	-2.489269
H	3.127898	2.855904	4.810821	C	-0.653234	-4.244938	0.130702
H	1.478984	5.139494	4.032679	C	3.522498	1.462607	-2.932092
H	3.157757	5.003188	3.528271	C	5.075229	2.060055	1.053779
H	1.912270	5.361544	2.347733	C	-2.019001	-3.196090	2.988843
H	-1.339113	5.039302	-0.296326	C	-4.620710	-2.045926	-0.249734
H	1.341445	5.039138	0.289410	C	-5.074996	-2.061740	1.053638
H	-0.909043	3.091343	-2.752753	C	-2.256048	-4.694938	3.216522
H	-3.128315	2.850113	-4.813748	I	-0.000073	-0.000752	2.581026
H	-1.398263	2.831305	-5.071553	N	1.052057	-2.924337	-0.223811
H	-2.166591	1.482317	-4.250900	C	2.429630	-2.592904	-0.516438
H	-1.911282	5.359108	-2.354784	C	3.297564	-2.332846	0.552438
H	-1.478476	5.134521	-4.039518	C	2.880856	-2.687042	-1.842173
H	-3.157141	4.999294	-3.534463	C	3.524990	-1.460081	2.931865
H	-4.530718	2.633063	-3.207692	C	3.201623	-3.907136	2.488662
H	-6.100646	1.980060	-1.448414	C	2.022569	-3.191204	-2.991150
H	-5.344880	1.828839	0.877146	C	4.622656	-2.041565	0.248889
H	-1.861812	2.158971	1.987659	C	4.219245	-2.395177	-2.082154
H	-3.203646	1.360011	3.775110	C	5.077185	-2.055742	-1.054425
H	-4.700461	1.604981	2.898487	C	2.271351	-2.448380	-4.305724
H	-3.563781	0.360489	2.379033	C	2.260865	-4.689694	-3.219845
H	-2.843531	3.854489	3.493448	H	1.510299	-2.723209	-5.030907
H	-2.578035	4.539932	1.898343	H	2.245292	-1.371670	-4.179380
H	-4.198296	4.069924	2.390622	H	3.232180	-2.711750	-4.739068
[Pt <sup>III</sup> ] 3				H	1.634830	-5.049982	-4.031970
Pt	-0.000003	0.000010	0.000100	H	3.297431	-4.874898	-3.489197
I	-0.000507	0.000796	-2.580830	H	2.039016	-5.286359	-2.341603
C	0.001041	-2.099054	-0.000693	H	0.979107	-3.050899	-2.727111
C	-0.001006	2.099072	0.000869	H	4.597958	-2.450291	-3.087814
N	1.049256	2.925351	0.223832	H	6.110211	-1.834205	-1.267447
				H	5.311203	-1.824737	1.046423
				H	1.808412	-2.354349	2.068024

H	3.405554	-0.447794	2.559136	C	2.023116	-0.659282	0.069961
H	3.066630	-1.519369	3.915537	C	-0.662650	-2.023482	0.077930
H	4.587405	-1.645692	3.065975	C	-2.580669	1.430327	1.031057
H	2.698329	-4.662930	1.892746	C	-3.901665	1.873923	1.028872
H	4.269936	-4.101648	2.437747	C	-4.734542	1.542236	-0.032078
H	2.886807	-4.032953	3.521529	C	-4.229340	0.774500	-1.073753
H	1.350517	-5.047017	-0.265131	C	-2.901174	0.354861	-1.037257
H	-1.345571	-5.048659	0.260009	Cl	-1.598956	1.848226	2.400978
H	-0.975708	-3.054740	2.724698	Cl	-4.520990	2.828358	2.331667
H	-2.033872	-5.290814	2.337836	Cl	-6.377920	2.077077	-0.055759
H	-1.629576	-5.055284	4.028286	Cl	-5.257846	0.356197	-2.399872
H	-3.292414	-4.881155	3.485945	Cl	-2.319466	-0.575981	-2.383243
H	-3.228602	-2.719062	4.737420	C	0.386539	2.881691	-1.071728
H	-1.506637	-2.729071	5.028804	C	0.807883	4.209126	-1.117885
H	-2.243163	-1.377616	4.178458	C	1.543922	4.732043	-0.062311
H	-4.595032	-2.457629	3.086588	C	1.843053	3.916846	1.022001
H	-6.108184	-1.841344	1.267056	C	1.399197	2.596025	1.033038
H	-5.309587	-1.828976	-1.046956	Cl	-0.501842	2.276835	-2.435746
H	-1.806352	-2.354760	-2.069493	Cl	0.430806	5.215009	-2.473695
H	-3.065160	-1.517936	-3.915889	Cl	2.080054	6.374777	-0.097439
H	-4.585711	-1.645560	-3.066105	Cl	2.758476	4.558260	2.342196
H	-3.403950	-0.448060	-2.558127	Cl	1.776797	1.637273	2.430670
H	-2.884310	-4.031840	-3.525070	C	2.560138	-1.382534	1.136731
H	-2.695543	-4.663845	-1.897105	C	3.880753	-1.825396	1.176327
H	-4.267354	-4.102355	-2.441294	C	4.731302	-1.542398	0.115148
H	-3.405190	0.445005	2.558112	C	4.243384	-0.823115	-0.968526
H	-3.067200	1.515056	3.915941	C	2.915068	-0.402183	-0.972661
H	-4.587791	1.641680	3.066075	Cl	1.555889	-1.739053	2.507431
H	-1.808860	2.352873	2.069693	Cl	4.478444	-2.719509	2.531109
H	-4.271164	4.098668	2.441239	Cl	6.374381	-2.077578	0.142597
H	-2.888191	4.029153	3.525172	Cl	5.293388	-0.466466	-2.295904
H	-2.699698	4.661301	1.897228	Cl	2.355863	0.465714	-2.369796
H	-4.597285	2.453845	-3.086592	C	-1.419058	-2.547468	1.127540
H	-6.110059	1.836284	-1.267180	C	-1.864269	-3.867296	1.168485
H	-5.311582	1.824418	1.046875	C	-1.548522	-4.730092	0.126707
H	-0.978425	3.053552	-2.724486	C	-0.794793	-4.255321	-0.939149
H	-1.509032	2.727986	-5.028657	C	-0.372938	-2.927399	-0.945860
H	-2.244830	1.375930	-4.178639	Cl	-1.817536	-1.526985	2.474837
H	-3.231007	2.716921	-4.737396	Cl	-2.801470	-4.448445	2.501043
H	-1.633502	5.053963	-4.027674	Cl	-2.085612	-6.372698	0.156321
H	-3.296229	4.878709	-3.485347	Cl	-0.396293	-5.321112	-2.242084
H	-2.037919	5.288873	-2.337162	Cl	0.538486	-2.384423	-2.320599
H	1.345781	5.048308	0.264814				
H	-1.350342	5.047410	-0.260150				
H	0.976714	3.052518	2.727039				
H	3.230111	2.714207	4.738772				
H	1.508243	2.724694	5.030725				
H	2.243905	1.373693	4.178919				
H	2.035436	5.288619	2.341878				
H	1.631538	5.051700	4.032233				
H	3.294175	4.877571	3.489263				
H	4.596078	2.454366	3.087234				
H	6.108461	1.839310	1.266625				
H	5.309021	1.829039	-1.047097				
H	1.805557	2.355889	-2.067984				
H	3.063866	1.521432	-3.915666				
H	4.584763	1.648872	-3.066489				
H	3.403792	0.450309	-2.559162				
H	2.882460	4.034938	-3.5222081				
H	2.693973	4.665102	-1.893372				
H	4.265818	4.104767	-2.438663				



Pt	-0.001629	0.000411	0.038159
C	-2.026501	0.660011	0.007064
C	0.659570	2.024783	-0.004105

## 7. EPR studies

### 7.1. Experimental details

The Electron Paramagnetic Resonance (EPR) spectra were measured in an Elexys E580E from Bruker. The modulation amplitude was currently 0.4 mT and the measuring temperature was in the 10 K to 80 K range. A liquid helium refrigerated Oxford CF900 continuous flow cryostat was employed for measurements at low temperatures. The temperature stability was better than 0.1 K.

Powdered polycrystalline samples of complex **3** were introduced in a quartz tube. In that case a preferential orientation was observed (see below) as a consequence of strong anisotropy of the gyromagnetic tensor. For obtaining randomly orientation spectra, the polycrystalline samples were dispersed in *n*-hexane and they were cooled down in absence of magnetic field to avoid preferential orientation in the field. However, orientation biased spectra let us to improve the resolution of the low field feature (see below).

### 7.2. Results and Analysis of the spectra

When a powdered polycrystalline sample is used for measuring the EPR spectra at low temperature no reproducible data were obtained. This behaviour is illustrated in figure S4 where the spectrum measured at 30 K after cooling the sample in absence of magnetic field and that recorded immediately, after the magnetic field reached a value of 1.4 T are shown. The changes observed in the spectrum are consequence of the bias of the orientation induced by the magnetic field that trend to orient the crystallites with the principal direction of the *g* tensor corresponding to the highest *g*-value parallel to the applied magnetic field.

To avoid this effect polycrystalline samples were dispersed in *n*-hexane and cooled down in absence of magnetic field. In this way complex **3** crystallites are immobilized in frozen *n*-hexane and then reproducible EPR spectra were obtained. Red trace in figure S5 show the EPR spectrum of a polycrystalline sample of complex **3** dispersed in *n*-hexane measured a 16 K.

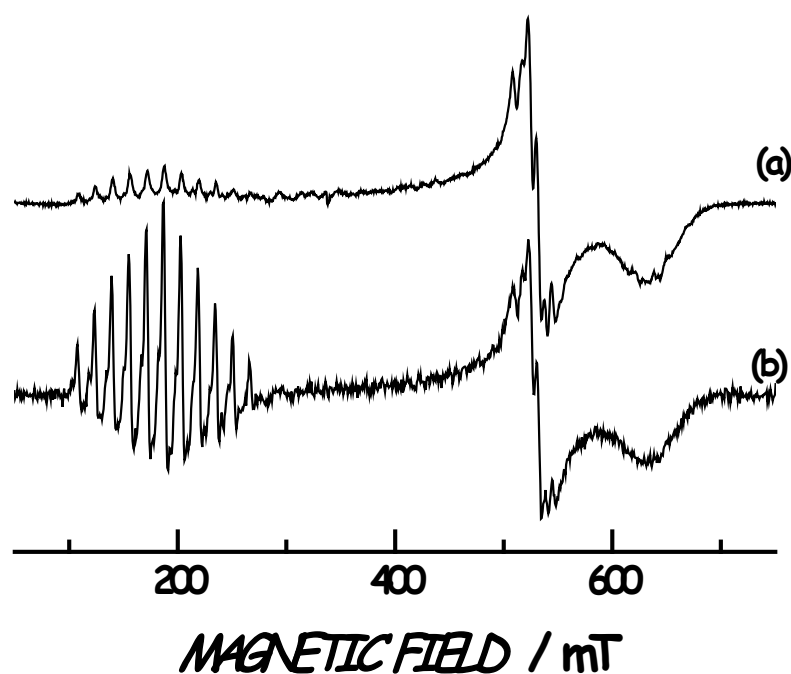


**Fig. S4** EPR spectra of a polycrystalline sample of complex **3** measured at 30 K. In all the cases the magnetic field strength increases as the measurement is recorded. (a) Initial spectrum after cooling down the sample in zero magnetic field. (b) Spectrum measured in the same conditions after taking the former spectrum; the magnetic field reached a value of 1.4 T.

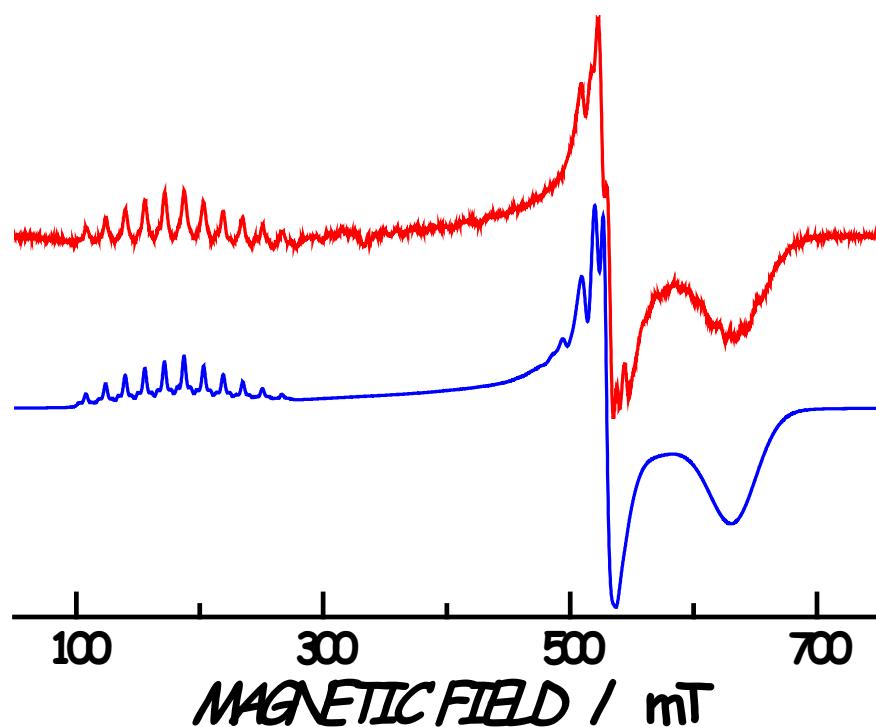


**Fig. S5** Red trace shows the EPR spectrum of a polycrystalline sample of complex **3** dispersed in *n*-hexane measured at 16 K. Blue trace represents the simulated spectrum calculated with *EasySpin* program.

The EPR spectra shown above correspond to an  $S = \frac{1}{2}$  entity with a markedly orthorhombic g-tensor. Besides the low field feature, corresponding to the contribution of crystallites oriented with their principal axis of the g-tensor associated to the highest principal g-value close to the magnetic field direction, shows a complex structure (see Fig. S6). It consists of eleven equally spaces (about 16 mT) with relative intensities following the sequence 1:2:3:4:5:6:5:4:3:2:1. They are marked by sticks. Besides, some weaker signals are observed in between, which are marked with stars. These last ones are more clearly resolved in the spectra of partially oriented samples and this last structure consists of two lines symmetrically distributed around the main lines with a splitting of about 9 mT among them.

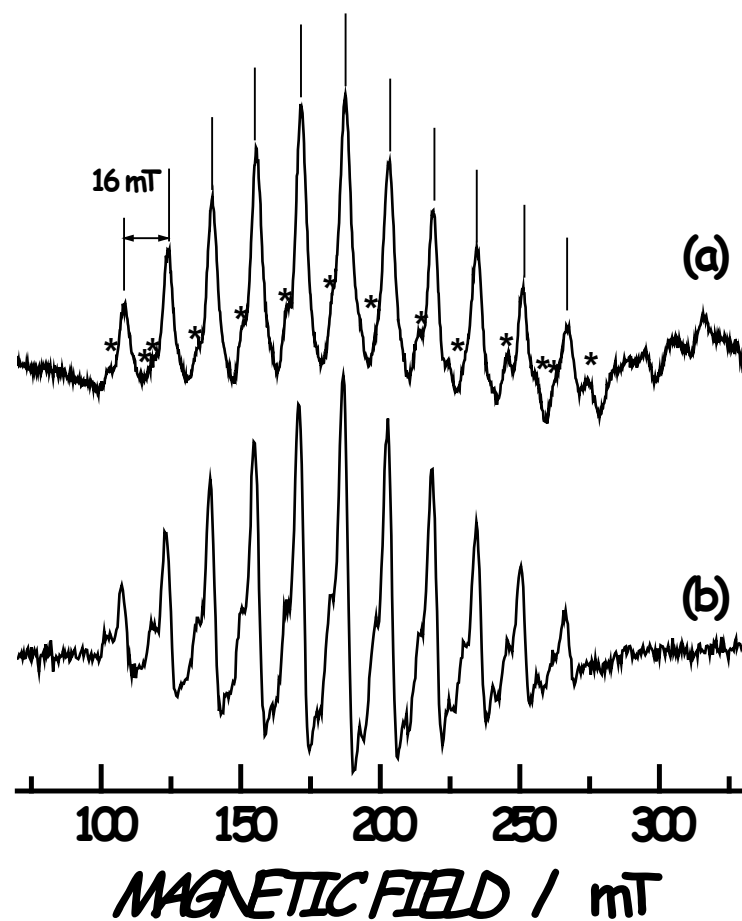


**Fig. S6** Detail of the low field feature region of the EPR spectra of complex 3 measured at 16 K. (a) polycrystalline sample dispersed in n-hexane. (b) partially oriented polycrystalline sample after the application of a magnetic field of 1.4 T.

Taking into account that iodine has a 100 % natural abundance isotope,  $^{127}\text{I}$ , with nuclear spin  $I = 5/2$  and considering the platinum moiety structure (see figure 2) the main structure of the low field feature is associated to the hyperfine interaction with two equivalent iodine nuclei. On the other hand  $^{195}\text{Pt}$  is the only natural isotope of platinum

(33.8 % natural abundance) with a non-null nuclear spin ( $I = \frac{1}{2}$ ). Therefore, the star marked signals in Fig. S6 could be associated to the hyperfine interaction with  $^{195}\text{Pt}$  nuclei.

Although some structure can be detected in the two high field features, the lack of resolution prevents us to make any definitive assignation. In any case, the effective interaction with the  $^{127}\text{I}$  for these orientations is sensibly lower and likely the same happens with the  $^{195}\text{Pt}$  hyperfine coupling. This lack of information prevents us a complete determination of all relevant hyperfine interaction parameters.

We have simulated some spectra with the help of *EasySpin* program<sup>13</sup> introducing some additional approximations in the description of the hyperfine interactions with the  $^{127}\text{I}$  and  $^{195}\text{Pt}$  nuclei. Firstly, we have assumed that the principal axes of all hyperfine tensors coincide with the principal axes of the *g*-tensors as it is suggested by the structure of the platinum moiety (see Fig. 2). Secondly, different values of the principal values of the hyperfine coupling tensor, low enough to keep the total width of the highest field features of the spectra, have been taken. Blue trace in figure S5 represents the calculated spectra with the following parameters.

$$\begin{array}{lll} g_1 = 1.069 & g_2 = 1.280 & g_3 = 3.612 \\ A_1(^{127}\text{I}) = 10 \text{ MHz} & A_2(^{127}\text{I}) = 10 \text{ MHz} & A_3(^{127}\text{I}) = 802 \text{ MHz} \\ A_1(^{195}\text{Pt}) = 125 & A_2(^{195}\text{Pt}) = 125 & A_3(^{195}\text{Pt}) = 500 \\ \text{MHz} & \text{MHz} & \text{MHz} \end{array}$$

Note that in this stage the values of  $A_1(^{127}\text{I})$ ,  $A_2(^{127}\text{I})$ ,  $A_1(^{195}\text{Pt})$  and  $A_2(^{195}\text{Pt})$  parameters are actually not determined and the former figures have to be read as a upper bound of their actual values.

## 8. Magnetic Measurements

### 8.1. Experimental details

Magnetic measurements were collected from a fine powdered polycrystalline samples, in a Quantum Design MPMS SQUID magnetometer, with the RSO high sensitivity option. The magnetometer was calibrated using standard palladium and dysprosium oxide reference samples supplied by Quantum Design. The accuracy of the measurements is better than 1%. The susceptibility data,  $\chi(T)$ , was taken from 1.8 to

280 K, with an applied d.c. external field of 1 kOe. Isothermal dc magnetization curves,  $M(\mu_0H)$ , at  $T = 1.8$  K were taken in the magnetic field range  $0 < \mu_0H < 5$  T.

### 8.2. Results and Analysis of the Data

The temperature dependence of the magnetic susceptibility of powdered polycrystalline samples of complex **3** is given in Fig. S7. It can be described by a Curie law,  $\chi(T) = C/T + \chi_0$ , where  $T$  is the temperature,  $C$  is the Curie constant, which can be derived from the EPR data ( $0.495 \text{ cm}^3 \cdot \text{K} \cdot \text{mol}^{-1}$ ) and  $\chi_0$  is a temperature-independent contribution. In that case a plot of the susceptibility,  $\chi(T)$ , as a function of the inverse of temperature should give a linear dependence as it is shown in the inset. Dashed lines in Fig. S7, which represent the calculated temperature dependence of magnetic susceptibility using this value of the Curie constant and  $\chi_0 = -1.2 \times 10^{-3} \text{ cm}^3 \cdot \text{K} \cdot \text{mol}^{-1}$ , account fairly good for the observed behavior.

The magnetization per formula unit, in Bohr magnetons,  $M/nN_A\mu_B$ , as a function of the reduced magnetic field,  $\mu_B H/k_B T$ , measured at 1.8 K for a polycrystalline sample of complex **3** is shown in Fig. S8. It shows a saturation trend corresponding to an  $S = \frac{1}{2}$  in keeping with a mononuclear low-spin  $d^7$  system.

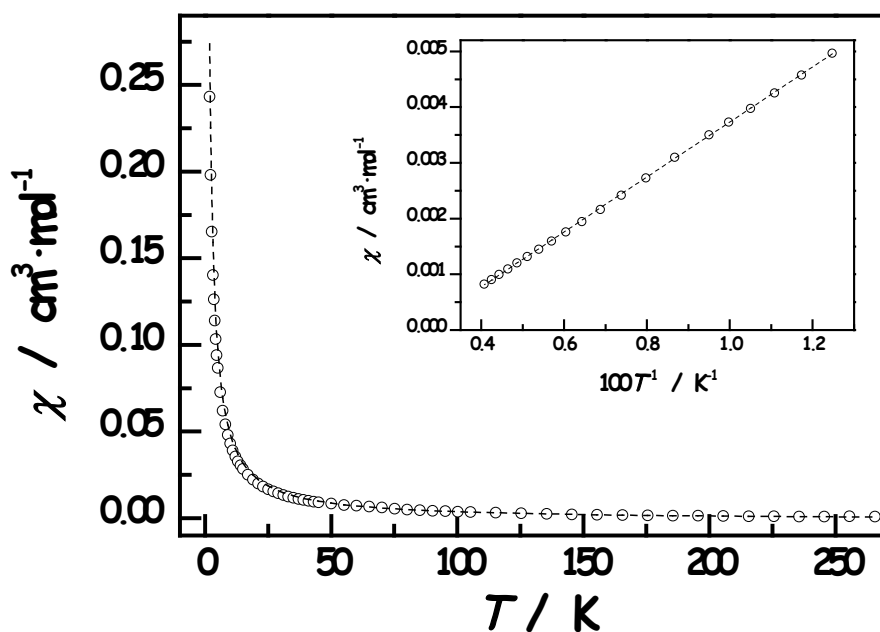


**Fig. S7** Temperature dependence of the molar susceptibility of complex **3** measured in a powdered sample between 1.8 and 270 K. Circles represents the experimental values and dashed line represents the evolution predicted by a Curie law (see text). The inset corresponds to a representation of the high temperature data ( $T > 80$  K) as a function of the reciprocal temperature.

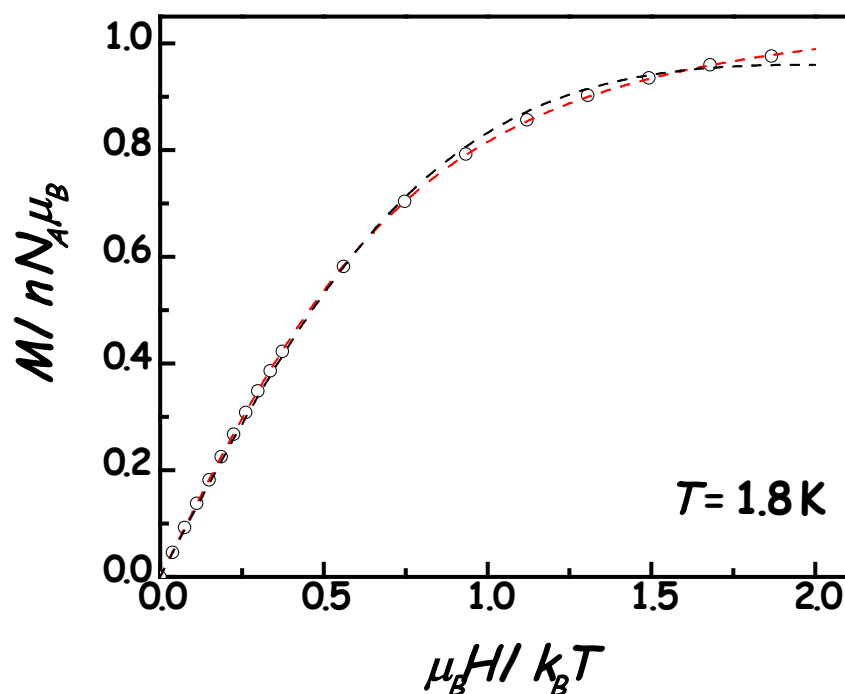


**Fig. S8** Circles give the magnetization per formula unit of a polycrystalline sample of complex **3** as a function of the reduced field,  $\mu_B H / k_B T$ , measured at 1.8 K. Dashed line corresponds to the predicted evolution using a Brillouin function considering an isotropic  $g$ -factor (black) and taking into account the anisotropy of the  $g$ -tensor (red).

If the  $g$ -tensor anisotropy is neglected, the dependence of the magnetization as a function of the reduced field is given by

$$\frac{M}{nN_A \mu_B} = gS \cdot B_S \left( gS \cdot \frac{\mu_B H}{k_B T} \right)$$

where  $B_S$  is the Brillouin function.<sup>14</sup>

Black dashed line in Fig. S8 represents the best fit of the former expression (with  $S = \frac{1}{2}$ ) to the experimental data obtaining by varying the  $g$ -factor. It corresponds to  $g = 2.228$ , giving a Curie constant value  $C = 0.466 \text{ cm}^3 \cdot \text{K} \cdot \text{mol}^{-1}$ . The disagreement of this value with the former quoted one, which explains the temperature dependence of the magnetic susceptibility, together with the failure in describing the whole dependence of the magnetization with the magnetic field point out that the  $g$ -anisotropy has to be taken into account.

Red dashed line in Fig. S8 corresponds to the evolution of the magnetization as a function of the reduced magnetic field calculated with an anisotropic  $g$ -tensor with its principal values derived from the EPR data following the procedure detailed by Bartolomé et al.<sup>15</sup> It fits fairly well to the experimental data.

## 9. X-Ray Crystal Structure Determination of Complexes **2** and **3**.

Crystals suitable for X-ray diffraction analysis were obtained from dichloromethane / diethyl ether (**2**) or dichloromethane / pentane (**3**) solvent system. The most relevant crystal and refinement data are collected in Tables S1 and S2.

In both cases, diffraction data were recorded on an Oxford Diffraction Xcalibur Nova (Agilent) single crystal diffractometer, using Cu-K $\alpha$  radiation ( $\lambda = 1.5418 \text{ \AA}$ ). Images were collected at a 63 mm fixed crystal-detector distance, using the oscillation method, with 1° oscillation and variable exposure time per image (5 – 15) and (30 – 60) s respectively. Data collection strategy was calculated with the program CrysAlis Pro CCD.<sup>16</sup> Data reduction and cell refinement was performed with the program CrysAlis Pro RED.<sup>16</sup> An empirical absorption correction was applied using the SCALE3 ABSPACK algorithm as implemented in the program CrysAlis Pro RED.<sup>16</sup>

The software package WINGX<sup>17</sup> was used for space group determination, structure solution and refinement. The structures of the complexes were solved by direct methods using SIR2004.<sup>18</sup>

In the crystal of complex **2** a C<sub>4</sub>H<sub>10</sub>O solvent molecule per unit formula of the complex is present. Isotropic least-squares refinement on F<sub>2</sub> using SHELXL97<sup>19</sup> was performed. During the final stages of the refinements, all the positional parameters and the anisotropic temperature factors of all the non-H atoms were refined. The H atoms were geometrically placed riding on their parent atoms with isotropic displacement parameters set to 1.2 times the U<sub>eq</sub> of the atoms to which they are attached (1.5 for methyl groups). The maximum residual electron density is located near to heavy atoms.

The function minimized was  $([\sum w F_O^2 - F_C^2]/\sum w(F_O^2)]^{1/2}$  where  $w = 1/[\sigma^2(F_O^2) + (aP)^2 + bP]$  ( $a = 0.0879$  and  $b = 0.0$  for **2** and  $a = 0.0758$  and  $b = 4.9860$  for **3**) from counting statistics and  $P = (\text{Max}(F_O^2, 0) + 2F_C^2)/3$ .

Atomic scattering factors were taken from the International Tables for X-Ray Crystallography International.<sup>20</sup>

9.1 X-Ray Crystal Structure Determination of Complexes 2 and 3. S15

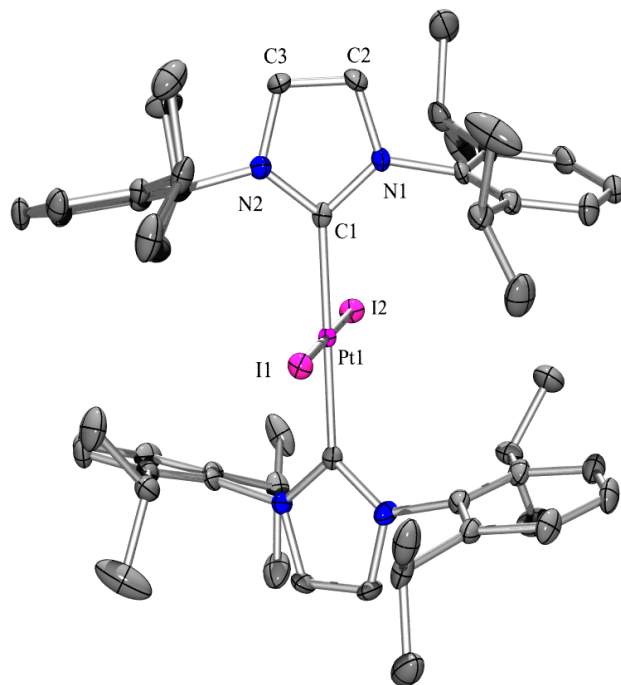


**Fig. S9** ORTEP-type view of complex 2. Thermal ellipsoids are drawn at 30% probability level. The molecule has crystallographically imposed twofold symmetry with the I1-Pt1-I2 and the oxygen atoms of the ether of solvation (not shown in this figure) located in the twofold axis. Selected bond lengths ( $\text{\AA}$ ): Pt1–C1: 2.024(7); Pt1–I1: 2.5948(9); Pt1–I2: 2.5974(7); C1–N1: 1.373(10); C1–N2: 1.354(11); N1–C2: 1.383(11); N2–C3: 1.401(11); C2–C3: 1.337(15).

9.2 Crystal data and structure refinement for compound 2.

**Table S1.** Crystal data and structure refinement for complex 2.

Identification code	orw335		
Empirical formula	C <sub>58</sub> H <sub>82</sub> I <sub>2</sub> N <sub>4</sub> O Pt		
Formula weight	1300.17		
Temperature	150(2) K		
Wavelength	1.54180 $\text{\AA}$		
Crystal system	Orthorhombic		
Space group	P 2 <sub>1</sub> 2 <sub>1</sub> 2 <sub>1</sub>		
Unit cell dimensions	$a = 10.6105(2)$ $\text{\AA}$	$\alpha = 90^\circ$ .	
	$b = 13.0106(2)$ $\text{\AA}$	$\beta = 90^\circ$ .	
	$c = 20.7461(4)$ $\text{\AA}$	$\gamma = 90^\circ$ .	
Volume	$2863.98(9)$ $\text{\AA}^3$		
Z	2		
Density (calculated)	1.508 Mg/m <sup>3</sup>		

Absorption coefficient	13.343 mm <sup>-1</sup>
F(000)	1300
Crystal size	0.193 x 0.123 x 0.052 mm <sup>3</sup>
Theta range for data collection	4.01 to 74.23°.
Index ranges	-12<=h<=9, -16<=k<=15, -25<=l<=11
Reflections collected	6821
Independent reflections	4885 [R(int) = 0.0699]
Completeness to theta = 74.23°	96.3 %
Refinement method	Full-matrix least-squares on F <sup>2</sup>
Data / restraints / parameters	4885 / 0 / 309
Goodness-of-fit on F <sup>2</sup>	1.026
Final R indices [I>2sigma(I)]	R1 = 0.0537, wR2 = 0.1366
R indices (all data)	R1 = 0.0645, wR2 = 0.1516
Absolute structure parameter	-0.006(13)
Largest diff. peak and hole	2.721 and -2.256 e.Å <sup>-3</sup>

### 9.3 Crystal data and structure refinement for compound 3.

**Table S2.** Crystal data and structure refinement for complex **3**.

Identification code	orw337
Empirical formula	C86 H84 B F24 I2 N4 Pt
Formula weight	2089.27
Temperature	100(2) K
Wavelength	1.54180 Å
Crystal system	Monoclinic
Space group	P 2/n
Unit cell dimensions	a = 19.6292(2) Å      α= 90°. b = 21.8184(2) Å      β= 94.328(1)°. c = 20.7055(2) Å      γ = 90°.
Volume	8842.42(15) Å <sup>3</sup>
Z	4
Density (calculated)	1.569 Mg/m <sup>3</sup>
Absorption coefficient	9.286 mm <sup>-1</sup>
F(000)	4132
Crystal size	0.087 x 0.077 x 0.028 mm <sup>3</sup>
Theta range for data collection	2.95 to 74.66°.
Index ranges	-22<=h<=18, -25<=k<=26, -25<=l<=24
Reflections collected	37621

Independent reflections	17385 [R(int) = 0.0391]
Completeness to theta = 67.00°	99.2 %
Absorption correction	Semi-empirical from equivalents
Max. and min. transmission	1.00000 and 0.52531
Refinement method	Full-matrix least-squares on F <sup>2</sup>
Data / restraints / parameters	17385 / 0 / 1081
Goodness-of-fit on F <sup>2</sup>	1.029
Final R indices [I>2sigma(I)]	R1 = 0.0452, wR2 = 0.1212
R indices (all data)	R1 = 0.0542, wR2 = 0.1311
Largest diff. peak and hole	2.214 and -1.900 e.Å <sup>-3</sup>

## 10. References

- 1 O. Rivada-Wheelaghan, B. Donnadieu, C. Maya and S. Conejero, *Chem. Eur. J.*, 2010, **16**, 10323.
- 2 N. A. Yakelis and R. G. Bergman, *Organometallics*, 2005, **24**, 3579.
- 3 (a) G. Gritzner and J. Kuta, *Pure Appl. Chem.*, 1984, **56**, 461; (b) N. G. Connally and W. E. Geiger, *Chem. Rev.*, 1996, **96**, 877.
- 4 (a) A. D. Becke, *J. Chem. Phys.*, 1993, **98**, 1372; (b) C. Lee, W. Yang and R. G. Parr, *Phys. Rev. B*, 1988, **37**, 785.
- 5 Gaussian 09, Revision B.01, M. J. Frisch, G. W. Trucks, H. B. Schlegel, G. E. Scuseria, M. A. Robb, J. R. Cheeseman, G. Scalmani, V. Barone, B. Mennucci, G. A. Petersson, H. Nakatsuji, M. Caricato, X. Li, H. P. Hratchian, A. F. Izmaylov, J. Bloino, G. Zheng, J. L. Sonnenberg, M. Hada, M. Ehara, K. Toyota, R. Fukuda, J. Hasegawa, M. Ishida, T. Nakajima, Y. Honda, O. Kitao, H. Nakai, T. Vreven, J. A. Montgomery, Jr., J. E. Peralta, F. Ogliaro, M. Bearpark, J. J. Heyd, E. Brothers, K. N. Kudin, V. N. Staroverov, R. Kobayashi, J. Normand, K. Raghavachari, A. Rendell, J. C. Burant, S. S. Iyengar, J. Tomasi, M. Cossi, N. Rega, J. M. Millam, M. Klene, J. E. Knox, J. B. Cross, V. Bakken, C. Adamo, J. Jaramillo, R. Gomperts, R. E. Stratmann, O. Yazyev, A. J. Austin, R. Cammi, C. Pomelli, J. W. Ochterski, R. L. Martin, K. Morokuma, V. G. Zakrzewski, G. A. Voth, P. Salvador, J. J. Dannenberg, S. Dapprich, A. D. Daniels, Ö. Farkas, J. B. Foresman, J. V. Ortiz, J. Cioslowski, and D. J. Fox, Gaussian, Inc., Wallingford CT, 2009.
- 6 (a) J. Poater, M. Sola, A. Rimola, L. Rodríguez-Santiago and M. Sodupe, *J. Phys. Chem. A*, 2004, **108**, 6072; (b) R. Ríos-Font, M. Sodupe, L. Rodríguez-Santiago and P. R. Taylor, *J. Phys. Chem. A*, 2010, **114**, 10857.

- 7 D. Andrae, U. Haeussermann, M. Dolg, H. Stoll and H. Preuss, *Theor. Chim. Acta*, 1990, **77**, 123.
- 8 A. W. Ehlers, M. Bohme, S. Dapprich, A. Gobbi, A. Hollwarth, V. Jonas, K. F. Kohler, R. Stegmann, A. Veldkamp and G. Frenking, *Chem. Phys. Lett.*, 1993, **208**, 111.
- 9 W. J. Hehre, R. Ditchfield and J. A. Pople, *J. Chem. Phys.*, 1972, **56**, 2257.
- 10 M. M. Francl, W. J. Pietro, W. J. Hehre, J. S. Binkley, M. S. Gordon, D. DeFrees and J. A. Pople, *J. Chem. Phys.*, 1982, **77**, 3654.
- 11 T. Clark, J. Chandrasekhar, G. W. Spitznagel and P. Schleyer, *J. Comput. Chem.*, 1983, **4**, 294.
- 12 P. J. Alonso, R. Alcalá, R. Usón and J. Forniés, *J. Phys. Chem. Solids*, 1991, **52**, 975.
- 13 S. Stoll and A. Schweiger, *J. Magn. Reson.*, 2006, **178**, 42.
- 14 R. Boča. *Theoretical Foundations of Molecular Magnetism*. Current Methods in Inorganic Chemistry; vol 1. Elsevier 1<sup>st</sup> edition (N.Y. 1999). Ch 6.
- 15 E. Bartolomé, P. J. Alonso, A. Arauzo, J. Luzón, J. Bartolomé, C. Racles and C Turta, *Dalton Trans.*, 2012, **41**, 10382.
- 16 *CrysAlis<sup>Pro</sup> CCD*, *CrysAlis<sup>Pro</sup> RED*. Oxford Diffraction Ltd., Abingdon, Oxfordshire, UK. (2008).
- 17 L. J. Farrugia, *J. Appl. Crystallogr.* 1999, **32**, 837.
- 18 M. C. Burla, R. Caliandro, M. Camalli, B. Carrozzini, G. L. Cascarano, L. De Caro, C. Giacovazzo, G. Polidori and R. Spagna, *J. Appl. Cryst.*, 2005, **38**, 381.
- 19 Sheldrick G. M. *SHELXL97: Program for the Refinement of Crystal Structures*; University of Göttingen: Göttingen, Germany, (2008).
- 20 *Tables for X-Ray Crystallography*; Kynoch Press, Birmingham, U.K., (1974); Vol. IV (present distributor: Kluwer Academic Publishers; Dordrecht, The Netherlands).